

This discussion paper is/has been under review for the journal *Atmospheric Chemistry and Physics (ACP)*. Please refer to the corresponding final paper in *ACP* if available.

# Investigation of downscaling techniques for the linkage of global and regional air quality modeling

Y. F. Lam and J. S. Fu

Dept. of Civil and Environmental Engineering, University of Tennessee, Knoxville, TN, USA

Received: 20 April 2009 – Accepted: 20 July 2009 – Published: 28 July 2009

Correspondence to: J. S. Fu (jsfu@utk.edu)

Published by Copernicus Publications on behalf of the European Geosciences Union.

ACPD

9, 16011–16050, 2009

## Techniques for global and regional air quality modeling

Y. F. Lam and J. S. Fu

Title Page

Abstract

Introduction

Conclusions

References

Tables

Figures

◀

▶

◀

▶

Back

Close

Full Screen / Esc

Printer-friendly Version

Interactive Discussion



## Abstract

Recent year, downscaling global atmospheric model outputs for the USEPA Community Multiscale Air Quality (CMAQ) Initial (IC) and Boundary Conditions (BC) have become practical because of the rapid growth of computational technologies that allow global simulations can be completed within a reasonable time and have better performance. The traditional method of generating IC/BC by profile data has lost its advocators due to the weakness of the limited horizontal and vertical variations found on the gridded boundary layers. In this paper, we are in effort to investigate the effects of using profile IC/BC and global atmospheric model data. We utilize the GEOS-Chem model outputs to generate time-varied and layer-varied IC/BC for year 2002 using our newly development of tropopause determining algorithm. The purpose of the study is to determine the tropopause effect to the downscaling process. From the results, we have found that without considering tropopause in the downscaling process created unrealistic O<sub>3</sub> concentrations in IC/BC at the upper boundary conditions for regional tropospheric model. This phenomenon has caused over-prediction of surface O<sub>3</sub> in CMAQ. And it is greatly affected by temperature and latitudinal location. With the implementation of our algorithm, we have successfully resolved the incompatibility issues in the vertical layer structure between global and regions chemistry models to yield better surface O<sub>3</sub> predictions than profile IC/BC on both summer and winter conditions. At the same time, it improved the vertical O<sub>3</sub> distribution of CMAQ outputs. The algorithm can be applied to a global atmospheric model which performs a reasonable outcome to determine the tropopause.

## 1 Introduction

Regional air quality models are designed to simulate the transport, production and destruction of atmospheric chemicals at the tropospheric level, where particular interest is given at the planetary boundary layer (PBL) that human activities reside (Byun and

## Techniques for global and regional air quality modeling

Y. F. Lam and J. S. Fu

Title Page

Abstract

Introduction

Conclusions

References

Tables

Figures

⏪

⏩

◀

▶

Back

Close

Full Screen / Esc

Printer-friendly Version

Interactive Discussion



Schere, 2006). Performance of the models depends greatly on the temporal and spatial quality of the inputs (i.e., emission inventories, meteorological model outputs and boundary conditions). Recent year, establishing proper boundary conditions (BCs) becomes a crucial process as the effects of intercontinental transport of air pollutants (Heald et al., 2003; Lin et al., 2008; Chin et al., 2007) and enhancement of background pollutants concentrations emerge (Vingarzan, 2004; Ordonez et al., 2007; Fiore et al., 2003). Various studies suggested that utilizing dynamic global chemical transport model (CTM) outputs as the BCs for the regional air quality model would be the best option for capturing the temporal variation and spatial distributions of the tracer species (Fu et al., 2008; Byun et al., 2004; Morris et al., 2006; Tang et al., 2007). For example, Song et al. (2008) applied the interpolated values from a global chemical model, RAQMS, as the lateral BCs for the regional air quality model, CMAQ and evaluated simulated CMAQ results with ozone soundings. Simulations were performed on the standard CMAQ seasonal varied profile BCs and dynamic BCs from RAQMS. The results demonstrated that dynamic BCs are necessary for simulating realistic vertical ozone profile on the regional air quality simulations.

The quality of BCs depends on the vertical, horizontal and temporal resolutions of global CTM outputs. The latitudinal location and seasonal effects are also playing an important role, which defines the tropopause height that influences the vertical interpolation process between global and regional models (Bethan et al., 1996; Stohl et al., 2003). In the MICS-Asia project, high ozone concentrations have been observed in BCs from the stratosphere during vertical interpolation process, as the regional model's layers reach above or beyond the tropopause height (Fu et al., 2008). These high values of ozone induced abnormality to the regional CTM simulation, as regional CTM is only designed for tropospheric application. Tang et al. (2008) studied various CTM lateral BCs from MOZART-NCAR, MOZART-GFDL and RAQMS. They observed that CTM BCs have induced high concentration of ozone in the upper troposphere in CMAQ, this high ozone aloft quickly have mixed down to the surface and resulting an overestimation of surface ozone. They have also concluded using outputs of the global CTM

---

## Techniques for global and regional air quality modeling

Y. F. Lam and J. S. Fu

---

[Title Page](#)[Abstract](#)[Introduction](#)[Conclusions](#)[References](#)[Tables](#)[Figures](#)[◀](#)[▶](#)[◀](#)[▶](#)[Back](#)[Close](#)[Full Screen / Esc](#)[Printer-friendly Version](#)[Interactive Discussion](#)

(GCTM) as BCs may not necessary better than the standard profile-BC and it strongly depended on location and time. The quick downward mixing in CMAQ has caused a bad prediction of surface ozone when both tropospheric and stratospheric ozone are included in the CTM BCs (Al-Saadi et al., 2007; Tang et al., 2007, 2008). Therefore, correctly defining tropopause height for separating troposphere and stratosphere becomes crucial to prevent stratospheric influence during the vertical interpolation process for CMAQ and other regional CTMs simulation.

The tropopause is defined as the boundary/transitional layer between the troposphere and the stratosphere, which separates by distinct physical regimes in the atmosphere. The height of tropopause ranges from 6 km to 18 km depended on seasons and locations (Stohl et al., 2003). Various techniques were developed for identifying the altitude of tropopause, which base on temperature gradient, potential vorticity (PV) and ozone gradient. In meteorological studies such as satellite and sonde data analysis, temperature gradient method, also referred as thermo tropopause method, is the most commonly used technique, at which searches the lowest altitude where the temperature lapse rate decreased to less than  $2^{\circ}\text{K}/\text{km}$ , for the next 2 km and defines as tropopause (WMO, 1986). In climate modeling, PV technique, referred as dynamic technique, is often applied to define tropopause. PV is a vertical momentum up drift parameter and is expressed by PV unit (PVU). The threshold value of tropopause lies between  $\pm 1.6$  to  $3.5$  PVU depended on the location in the globe (Hoinka, 1997). Recently, attempt of improving regional model (i.e. pure tropospheric model), CMAQ, to simulate ozone at the lower stratosphere was performed using Potential Vorticity relationship. Location independent correlation between PVU with ozone concentrations was applied to correct the near/above-tropopause ozone concentrations in CMAQ. The fundamental disadvantage of using such technique is the implementation of a single correlation profile (i.e.  $R^2=0.7$ ) to represent the entire study domain (i.e. Continental USA). It notices that a slight shift of PV value in the profile could result a big change of ozone concentration, up to 100 ppbv. In addition, this profile may not applicable for all locations in the domain due to limitation of the literature data (Mathur et al., 2008). In

---

**Techniques for global and regional air quality modeling**Y. F. Lam and J. S. Fu

---

[Title Page](#)[Abstract](#)[Introduction](#)[Conclusions](#)[References](#)[Tables](#)[Figures](#)[◀](#)[▶](#)[◀](#)[▶](#)[Back](#)[Close](#)[Full Screen / Esc](#)[Printer-friendly Version](#)[Interactive Discussion](#)

GCTM downscaling, ozone gradient technique, referred as ozone profile technique, is more appropriate for defining tropopause since we have observed stratospheric level of ozone (i.e. about 300 ppbv) at the level of thermo and dynamic tropopause (Lam et al., 2008).

5 Ozone tropopause is defined by atmospheric ozone concentration, which observes a sharp transition from low concentrations to high concentrations from troposphere to stratosphere. The defined O<sub>3</sub> tropopause is consistently lower than the thermal and dynamic tropopause (Bethan et al., 1996).

10 The height of tropopause affects both the stratosphere-troposphere exchange (STE) as well as the transport of O<sub>3</sub> at upper troposphere (Holton et al., 1995; Stohl et al., 2003). In global CTM, well-defined vertical profiles of troposphere, tropopause and stratosphere are established for simulating STE, upper tropospheric advection and other atmospheric processes. Collins (2003) estimated that the net O<sub>3</sub> flux from stratosphere could contribute 10 to 15 ppbv of the overall tropospheric ozone (Collins et al., 15 2003). Moreover, the transport of O<sub>3</sub> is found much higher in upper troposphere than at lower troposphere, which relates to the long lifetime of O<sub>3</sub> and the high advective wind in upper troposphere. The advantage of employing CTM outputs as BCs gives a better representation of upper troposphere and the effect of STE can be taken into account. Since the global CTM is not intended to describe detailed surface flux conditions with 20 high spatial and high tropospheric resolutions, therefore, the regional air quality model is remained indispensable for simulating PBL conditions.

25 In this study, we have developed a linking tool to provide lateral BCs of the USEPA Community Multiscale Air Quality (CMAQ) model with the outputs from GEOS-Chem (Byun and Schere, 2006; Lam et al., 2008; Li et al., 2005). One full year of GEOS-Chem data in 2002 are analyzed and summarized to explore the seasonal variations of O<sub>3</sub> vertical profiles and tropopause heights in global CTM with available ozonesonde data in US are used to verify the performance of GEOS-Chem model. Evaluations are conducted on potential impact of changing tropopause height to the performance of the interpolated BCs toward the regional CTM. A new algorithm, “tropopause-determining

---

## Techniques for global and regional air quality modeling

Y. F. Lam and J. S. Fu

---

[Title Page](#)[Abstract](#)[Introduction](#)[Conclusions](#)[References](#)[Tables](#)[Figures](#)[◀](#)[▶](#)[◀](#)[▶](#)[Back](#)[Close](#)[Full Screen / Esc](#)[Printer-friendly Version](#)[Interactive Discussion](#)

algorithm” is proposed for the vertical interpolation process during downscaling to remove stratospheric effects from the global CTM toward the regional CTM. Verifications of the new approach are performed using three sets of CMAQ simulations, which are 1) the static lateral BCs from predefined profile. This BCs is used as a experimental control for GEOS-Chem data inputs; 2) standard dynamic lateral BCs from GEOS-Chem using original vertical interpolation; and 3) the modified dynamic lateral BCs from GEOS-Chem based on the new algorithm, and is intended to show the improvement of the proposed idea using the observation data from ozonesonde and CASTNET. Moreover, it demonstrates the necessity of filtering the tropospheric portion of global GMC outputs for the inputs in regional air quality modeling.

## 2 Description and configuration of models used

In this study, GEOS-Chem global chemistry model output is used to provide lateral boundary conditions for the regional air quality model CMAQ, where meteorological inputs are driven by MM5 mesoscale model. The model setups are described as follow.

## 3 GEOS-Chem

GEOS-Chem global chemistry model output is one of the most popular global models for generating BCs for the CMAQ regional model (Tesche et al., 2006; Morris et al., 2005; Streets et al., 2007; Tagaris et al., 2007; Eder and Yu, 2006) Many studies demonstrated that GEO-Chem is capable of capturing the effects from intercontinental transport of air pollutants and increasing background concentrations (Heald et al., 2006; Liang et al., 2007; Park et al., 2003) GEOS-Chem is a hybrid (stratospheric and tropospheric) 3-D global chemical transport model with coupled aerosol-oxidant chemistry (Park et al., 2006). It uses 3-h assimilated meteorological data such as winds, convective mass fluxes, mixed layer depths, temperature, clouds, precipitation,

## Techniques for global and regional air quality modeling

Y. F. Lam and J. S. Fu

Title Page

Abstract

Introduction

Conclusions

References

Tables

Figures

◀

▶

◀

▶

Back

Close

Full Screen / Esc

Printer-friendly Version

Interactive Discussion



and surface properties from the NASA Goddard Earth Observing System (GEOS-4) to simulate atmospheric transports and chemical balances. In this study, all GEOS-Chem simulations were carried out with 2° latitude by 2.5° longitude (2°×2.5°) horizontal resolution on 48 sigma vertical layers. The lowest model levels are centered at approximately 10, 50, 100, 200, 400, 600, 900, 1200, and 1700 m above the surface. A full-year simulation was conducted for year 2002, which were initialized on 1 September 2001 and continued for 16 months. The first four months were used to achieve proper initialization, and the following 12 months were the actual simulation results. Detailed discussion of GEOS-Chem is available elsewhere (Park et al., 2004).

For the purpose of developing a new algorithm for the downscaling linkage application, the outputs from GEOS-Chem in 2002 were being analyzed for investigating the variation of tropopause heights. In literature, many studies have already demonstrated the ability of GEOS-Chem to predict ozone vertical profile using ozonesonde and satellite observations (Liu et al., 2006; Fusco and Logan, 2003; Martin et al., 2002), therefore, in here, no detailed performance analysis would be conducted. Note that GEOS-Chem simulates stratospheric ozone with the Synoz algorithm (McLinden et al., 2000), which gives us the right cross-tropopause ozone flux but no guarantee of correct ozone concentrations in the region. That's because, until recently cross-tropopause transport of air in the GEOS fields was sometimes too fast. This is discussed for example in Bey et al. (2001), Liu et al. (2001), Fusco and Logan (2003). Nevertheless, for this study, simple model verifications were still conducted on the GEOS-Chem outputs using available ozonesonde data in US (Newchurch et al., 2003). Particular interests were given to upper troposphere and tropopause regions (1000 hPa to 1 hPa), where downscaling process could influence by stratospheric ozone. Figure 1 shows the yearly variability of GEOS-Chem with ozonesonde data. It is observed that 99.5% of GEOS-Chem outputs are contained within the statistical range of the observation data, which gives a good indication of reasonable model results. For the Boulder and Huntsville sites, good model performances were found at higher pressure when the pressure fell between 1000 hPa to 300 hPa. Consistent under-predictions were observed at the upper

---

## Techniques for global and regional air quality modeling

Y. F. Lam and J. S. Fu

---

[Title Page](#)[Abstract](#)[Introduction](#)[Conclusions](#)[References](#)[Tables](#)[Figures](#)[⏪](#)[⏩](#)[◀](#)[▶](#)[Back](#)[Close](#)[Full Screen / Esc](#)[Printer-friendly Version](#)[Interactive Discussion](#)

atmosphere when the pressures dropped below 250 hPa.

#### 4 MM5 and CMAQ

The CMAQ meteorological inputs are driven by NCAR's 5th generation Mesoscale Model version 3.7 (MM5) with hourly temporal resolution, 36 km horizontal resolution, and 34 sigma vertical layers. All MM5 simulations were conducted using one-way nested approach from 108 km over North America (140–40° W, 10–60° N) down to 36 km continental US (128–55° W, 21–50° N). For meteorological initial and boundary conditions, the NCEP Final Global Analyses (FNL) data (i.e. ds083.2) with resolution of 1° by 1° from the US National Centers for Environmental Prediction (NCEP) was used. For MM5 simulations, 4-D analysis nudging technique was employed to reproduce the observed weather conditions using the surface and upper layers observations from DS353.4 and DS464.0, respectively. The new Kain-Fritsch cumulus, Mix-phase micro-physic, RRTM long-wave radiations, planetary boundary layer (PBL) and land surface model (LSM) were configured in the simulations. A detailed summary of MM5 configuration is listed in Table 1. For CMAQ, Lambert conformal projection with true latitude limits of 25 and 40 was used on 148 by 112 grid cells with horizontal resolution of 36 km. The center of the domain was set at 100° W and 40° N. This domain covers entire continental US with part of the Mexico and Canada as referred as CONUS domain, which is shown in Fig. 2. In CMAQ simulations, three scenarios with different lateral boundary conditions were performed, which were profile boundary conditions (Profile-BC), ordinary vertical interpolated GEOS-Chem boundary conditions (ORDY-BC) and vertical interpolated GEOS-Chem boundary conditions using the new algorithm (Tropo-BC). All these simulations were configured with Carbon Bond IV (CB-IV) chemical mechanism with aerosol module (AERO3). Detailed configuration is also shown in Table 1.

### Techniques for global and regional air quality modeling

Y. F. Lam and J. S. Fu

Title Page

Abstract

Introduction

Conclusions

References

Tables

Figures

◀

▶

◀

▶

Back

Close

Full Screen / Esc

Printer-friendly Version

Interactive Discussion



## 5 Linkage methodology between GEOS-Chem and CMAQ

The GEOS-Chem outputs were extracted as CMAQ lateral boundary conditions using GEOS2CMAQ linkage tool that we have developed and will describe in the next section, which involved grid structure association, horizontal/vertical interpolation and chemical mapping processes. In the linkage process, GEOS2CMAQ applied the “nearest neighbor” method to associating the latitude/longitude formatted GEOS-Chem outputs with the CMAQ Lambert Conformal girded format. Horizontal interpolating process then utilized the results to interpolate the GEOS-Chem outputs into CMAQ girded format for each vertical layer column. For Tropo-BC, a newly developed tropopause-determining algorithm was implemented in the vertical interpolating process to define the tropopause height. Moreover, it separated the troposphere from the stratosphere for each horizontal grid. Different interpolating processes were enforced in the tropospheric and the stratospheric regions. Detailed discussion will be on latter section. For the chemical mapping process, 37 GEOS-Chem species were transformed into 30 CB-IV mechanism species of CMAQ according to the chemical definitions given in Appendix A. The GEOS-Chem species with the same definitions as CB-IV species were mapped directly into CMAQ; where as other species were mapped by partitioning and/or regrouping processes. For example, total oxidants  $O_x$  species in GEOS-Chem were defined as the combination of  $O_3$  and  $NO_x$ . Therefore, to obtain  $O_3$  concentrations,  $O_x$  was subtracted by  $NO_x$  species in GEOS-Chem. Other species, such as paraffin carbon bond (PAR), were composed of multiple species in GEOS-Chem. Regrouping was required to reconstruct the CB-IV corresponding species, which is shown as follows:

$$PAR = \frac{1}{4}ALK4 + \frac{1}{3}C_3H_8 + \frac{10}{4}C_2H_6 + \frac{1}{3}ACET + \frac{1}{4}MEK + \frac{1}{2}PREPE \quad (1)$$

For chemicals that were not supported by GEOS-Chem, CMAQ predefined boundary conditions, were used to maintain full list of CMAQ CB-IV species.

### Techniques for global and regional air quality modeling

Y. F. Lam and J. S. Fu

Title Page

Abstract

Introduction

Conclusions

References

Tables

Figures

◀

▶

◀

▶

Back

Close

Full Screen / Esc

Printer-friendly Version

Interactive Discussion



## 6 Tropopause determining algorithm

The newly developed tropopause-determining algorithm was added to the ordinary interpolating process (i.e. uses pressure level as only criteria in the interpolating process) for handling the near tropopause and stratosphere interpolating processes, which essential to correct and represent the global model outputs in regional model. We have utilized the ozone tropopause definition described in Bethan (1996), instead of thermo and dynamic tropopause definitions, as the basis for separating the stratosphere and the troposphere. Although thermo and dynamic tropopause are more commonly used in determining the tropopause, we have identified that these tropopause are inappropriate for this application because of observed stratospheric ozone effect at the troposphere. Since the purpose of determining tropopause is to use for excluding stratospheric pollutants concentrations from the global model during the interpolating process, ozone tropopause is better suited for this application. Ozone tropopause is defined as the location at which abrupt change of ozone concentration occurred. Our algorithm finds the ozone tropopause by finding the largest negative rate of change of slope (i.e. could be negative) from the plot of elevation verses ozone concentration. In other word, we have taken the second derivative of elevation with respect to ozone concentration and find the lowest value.

$$H_{\text{Tropo}(C_i)} = \max \left| \frac{C_{i+1} - C_i}{H_{i+1} - H_i} - \frac{C_i - C_{i-1}}{H_i - H_{i-1}} \right| \quad \text{where } 8 \text{ km} < H < 19 \text{ km} \quad (2)$$

Each rate of change of slope requires 3 data points or 2 line segments, which two line slopes were calculated. In tropopause level, which indicated by the largest negative rate of change of slope, a combination of a small concentration change in the first segment with a large concentration change in the second segment were obtained. Occasionally, a false tropopause was identified when extremely small change of ozone concentration in the first segment or negative change of ozone concentrations in the second segment was occurred. To ensure the tropopause found by this method is a reasonable tropopause height with no stratospheric effect, we have cross check

### Techniques for global and regional air quality modeling

Y. F. Lam and J. S. Fu

Title Page

Abstract

Introduction

Conclusions

References

Tables

Figures

◀

▶

◀

▶

Back

Close

Full Screen / Esc

Printer-friendly Version

Interactive Discussion



the tropopause results with thermo tropopause heights (i.e. ozone tropopause should be lower than thermo tropopause), as well as the maximum concentrations of ozone should be exceeded 300 ppbv found in literature (McPeters et al., 2007).

For the vertical interpolating process in GEOS2CMAQ, stratospheric ozone is excluded by limiting the maximum ozone concentration at the tropopause level while generating CMAQ lateral boundary conditions. Unlike some of the studies, without enforcing any upper bound limit or using predefined maximum ozone concentration, we have dynamically determined the altitude of the tropopause for each grid and time-step in GEOS-Chem outputs for use in vertical interpolating process (Morris et al., 2006; Song et al., 2008; Tang et al., 2007).

## 7 Results and discussion

### 7.1 CMAQ lateral boundary conditions

We have generated CMAQ lateral boundary conditions from every third hour GEOS-Chem outputs for VISTAS CMAQ simulation using GEOS2CMAQ linkage tool. In Fig. 3, comparisons of Profile-BC, ORDY-BC and Tropo-BC for 22 June 2002 is shown on CONUS domain. The top row represents the 1st CMAQ layer (~1000 mbar) and the bottom shows the top CMAQ layer (i.e. 19th layer ~140 mbar). These plots are intended to demonstrate the horizontal distribution of ozone concentrations across CONUS domain. The Profile-BC was designed to represent the relatively clean air conditions for CONUS boundaries. It enforces a pre-defined vertical profile with no tempo and spatial dependences. In general, the surface ozone concentrations (i.e. 1st layer) are ranged between 30 to 35 ppbv and it progressively increases and reaches a peak ozone concentration of 70 ppbv at the top (i.e. 19th layer). The ORDY-BC and Tropo-BC were both generated using the linkage methodology described early. This methodology intends to incorporate the effects of intercontinental transports of air pollutants and rising in background ozone concentrations into CMAQ by utilizing GEOS-Chem outputs (Bertschi et

Title Page

Abstract

Introduction

Conclusions

References

Tables

Figures

◀

▶

◀

▶

Back

Close

Full Screen / Esc

Printer-friendly Version

Interactive Discussion



al., 2004; Fiore et al., 2003; Park et al., 2004). The tempo and horizontal variations in GEOS-Chem were captured into CMAQ to reflect daily diurnal differences in concentrations. In ORDY-BC and Tropo-BC, the difference was the vertical interpolating process. ORDY-BC uses the ordinary vertical interpolating process, whereas Tropo-BC uses the ordinary vertical interpolating process with tropopause-determining algorithm that excludes pollutants in stratosphere from interpolating process. In the surface level (1st layer), both ORDY-BC and Tropo-BC perform identical and ozone concentrations are ranged from 19 ppbv to 90 ppbv depended on location and time in 22 June. For other days in 2002 (i.e. January, June and July), ozone concentration could reach up to 130 ppbv at the surface. In the top level (19th layer), the ORDY-BC ozone reaches as much as 235 ppbv and the Tropo-BC ozone achieves up to 160 ppbv in CONUS domain in 22 June. For other days in 2002, the ORDY-BC and Tropo-BC ozone reach up to 714 ppbv and 205 ppbv, respectively. In Considine (2008), the reported maximum mean tropopause ozone concentration from observations in North America is about 235 ppbv based on thermo tropopause definition. We would expect that if the Considine's analyzes use the ozone tropopause as definition, the maximum tropopause ozone concentrations should be lower since the ozone tropopause is constantly lower than the thermo tropopause at upper troposphere. So, the maximum ORDY-BC ozone of 714 ppbv would be too high in the troposphere and would impractically bring high ozone to surface level, whereas the maximum Tropo-BC ozone of 205 ppbv is fallen within reasonable value in US. It should be noted that the Considine's data is concentration at higher latitudinal locations. With the direct proportional relationship between latitudinal location and tropopause ozone concentration, we would expect that the reported 235 ppbv should be a high end of the ozone concentration at the tropopause in US.

As tests of the lateral boundary conditions responses to the GEOS2CMAQ linkage tool, we have extracted the vertical profiles of various CMAQ boundary conditions for selected months to investigate the seasonal effects of the data. Figure 4 shows average monthly ozone vertical distribution from all four boundaries of the CONUS domain:

---

## Techniques for global and regional air quality modeling

Y. F. Lam and J. S. Fu

---

[Title Page](#)[Abstract](#)[Introduction](#)[Conclusions](#)[References](#)[Tables](#)[Figures](#)[⏪](#)[⏩](#)[◀](#)[▶](#)[Back](#)[Close](#)[Full Screen / Esc](#)[Printer-friendly Version](#)[Interactive Discussion](#)

East, West, South and North are shown in various colors with average vertical temperature profiles for January, June and July. January represents the winter condition where tropopause is relatively low as consequence of cold temperature; July characterizes as the summer condition with possible high surface ozone concentration; Additional month of June is selected because we have occasionally observed high tropopause effects to the surface ozone from the MISC-ASIA study (Fu et al., 2008). As expected, Profile-BC on the left have shown no seasonal variation. In contrast, the ORDY-BC and Tropo-BC are both showing strong seasonal dependence. The ORDY-BC in the middle panel has shown a strong seasonal difference at the top CMAQ layer (i.e. blue line). This dependence directly relates to the seasonal difference in ozone tropopause heights as result of temperature differences. In ORDY-BC interpolating process, the amount of stratospheric ozone included in boundary conditions is governed by the altitude of ozone tropopause. It is highly sensitive with elevation because ozone is exponentially increased with altitude beyond tropopause or at stratosphere. The vertical structures of CMAQ and GEOS-Chem are also playing an important role. With the constant elevations in CMAQ layers, the higher tropopause is located, the less stratospheric effect will result. As shown in Fig. 4, the monthly average ozone concentrations for ORDY-BC on North bound at the top CMAQ layer for January, June and July are 362 ppbv, 207 ppbv and 172 ppbv, respectively. As recalled from early comparisons with Considine (2008), this average concentration in January is too high. For Tropo-BC, in which shown on the right panel, little seasonal variation is observed at the top CMAQ layer. The average monthly ozone concentrations of 94 ppbv, 90 ppbv and 86 ppbv are found on the south bound for January, June and July, respectively. These results demonstrate the effects of tropopause-determining algorithm, which have limited the stratospheric effects from the BCs.

In addition to the seasonal effect, latitudinal effect is also observed in Fig. 4, where South bound (i.e. downward triangle in black) has the highest concentration and the north bound (i.e. upward triangle in blue) exhibits the lowest concentration at the upper CMAQ layers (top two layers) on both ORDY-BC and Tropo-BC. The latitudinal effect is

---

## Techniques for global and regional air quality modeling

Y. F. Lam and J. S. Fu

---

[Title Page](#)[Abstract](#)[Introduction](#)[Conclusions](#)[References](#)[Tables](#)[Figures](#)[◀](#)[▶](#)[◀](#)[▶](#)[Back](#)[Close](#)[Full Screen / Esc](#)[Printer-friendly Version](#)[Interactive Discussion](#)

mainly induced by the temperature differences at troposphere on different boundaries. The vertical temperature profile in CMAQ on the right shows a decrease in temperature with increase in elevation and no temperature inversion is observed. This indicates all CMAQ layers are fallen within troposphere because it illustrates a tropospheric laps rate pattern.

## 7.2 CMAQ outputs

The CMAQ model was used to simulate the surface ozone concentrations in 36 km CONUS domain using Profile-BC, ORDY-BC and Tropo-BC with VISTAS emissions inventories (Morris et al., 2006). Figure 5 shows the CMAQ simulated vertical distribution of monthly ozone in Boulder, CO, Huntsville, AL and Trinidad head, CA with available ozonesonde for months of January, June and July. In the plot, the elevation is taken from the mid-point of each CMAQ layer. It should be noted that CMAQ is a tropospheric model. Therefore, the maximum concentration of ozone should not exceed the reported maximum tropopause concentration of 235 ppbv. It is observed that ORDY-BC (i.e. in black triangle) overestimates the January ozone concentrations for all locations in all altitudes (i.e. top panels). Moreover, overestimations are also observed in June at Boulder (i.e. middle left panel) and Trinidad Head at upper altitude (i.e. middle right panel). The overestimations in ORDY-BC are mainly resulted from bad lateral boundary conditions (i.e. unreasonable ozone concentration at the troposphere) propagated through downscaling process. By removing stratospheric ozone from ORDY-BC, which demonstrated by Tropo-BC, CMAQ outputs have shown a much better result when comparing with ozonesonde. For Profile-BC, similar results as Tropo-BC are observed; Slight extra overestimations are found in January and slight extra underestimations are found in June and July when comparing with Tropo-BC. Overall, Tropo-BC shows the best agreement with ozonesonde data. It should be noted that the underestimations in Huntsville in July are unrelated to the selection of lateral BCs since very little differences are observed among different lateral BCs. The underestimations in here revive that CMAQ model is incapable of simulating the upper ozone concentration in the area

## Techniques for global and regional air quality modeling

Y. F. Lam and J. S. Fu

Title Page

Abstract

Introduction

Conclusions

References

Tables

Figures

◀

▶

◀

▶

Back

Close

Full Screen / Esc

Printer-friendly Version

Interactive Discussion



where large change of upper ozone concentration are occurred. We believed that this may be resolved if CMAQ can implement STE mechanism along with supplementary upper boundary condition from GCM.

Figures 6 and 7, respectively, show the outputs of the average monthly surface ozone concentrations and the maximum monthly surface ozone concentrations for January (top frames), June (middle frames) and July (bottom frames). The maximum ozone concentrations within the domain are also listed at the corner and denoted in blue or white. In Fig. 6, the output results show that similar ozone concentration patterns are found across CONUS domain among all three BCs with some exceptional high ozone is observed in the ORDY-BC. It is believed that these high ozone concentrations occurring in the Western US in ORDY-BC are the consequence of high ozone observed at the top layer of CMAQ boundaries discussed early. The undesirable boundary conditions (i.e. ORDY-BC) produce abnormal surface ozone concentrations for both January and June. Since ozone is a photochemical pollutant driven by  $\text{NO}_x$ , VOCs and temperature, we would expect higher monthly average ozone should be observed in July than January. In the top frames, the reported maximum average ozone concentrations in January for Profile-BC, ORDY-BC and Tropo-BC are 55 ppbv, 69 ppbv and 50 ppbv, respectively. Similar trend is observed for June. For July (bottom frames), due to the tropopause is much higher than other months at the top layer, the effects of stratospheric ozone in ORDY-BC become minimal. As a result, fewer differences are founded among these three scenarios. Figure 7 shows that the monthly maximum 8-h ozone concentration in January on ORDY-BC is in excess of 150 ppbv over Western US. The result indicates that the effect of stratospheric ozone in lateral boundary conditions have significant impact on surface ozone concentrations, as a result of the high ozone aloft mix downward quickly. The large differences observed between ORDY-BC and Profile-BC/Tropo-BC reveal an important message, which is “excluding stratospheric ozone on tropospheric model during downscaling process is extremely important”. We have found the concentration differences between these scenarios could be as much as 87 ppbv in January. These differences gradually decrease with temperature increasing

---

## Techniques for global and regional air quality modeling

Y. F. Lam and J. S. Fu

---

[Title Page](#)[Abstract](#)[Introduction](#)[Conclusions](#)[References](#)[Tables](#)[Figures](#)[⏪](#)[⏩](#)[◀](#)[▶](#)[Back](#)[Close](#)[Full Screen / Esc](#)[Printer-friendly Version](#)[Interactive Discussion](#)

through June and July. The effects of lateral BCs in ORDY-BC have contributed to the high surface concentrations observed in Western US. Since both ORDY-BC and Tropo-BC utilize dynamic algorithm to interpolate the vertical ozone profile for each horizontal grid for lateral BCs, the variations in the western boundary are observed. Note that the Tropo-BC is intended to demonstrate the effectiveness of the tropopause-determining algorithm of separating the stratospheric and tropospheric ozone for lateral boundary condition.

### 7.3 CMAQ performance analyses

Model performance analyzes on all three cases have been performed using entire CASTNET dataset, in which 70+ observation sites across CONUS domain from both EPA and National Park Service (NPS) are included. It should note that our study only simulates 36 km domain and it is intended to demonstrate the effects of different BCs. Hence, the results in root mean square error in this research may be higher than the one in a finer resolution CMAQ. Figure 8 shows the simulated and measured surface ozone for months of January, June and July at the nearest locations of the ozonesonde sites found in CASTNET network (see Fig. 2 denoted in red star). In the plot, blue, purple, green and red colors are corresponding to observation, Profile-BC, ORDY-BC and Tropo-BC, respectively. And the top, middle and bottom panels show the first 15 days outputs for January, June and July, respectively. It should note that, due to limitation of the size of plot, we have only documented the first 15 days of date in Fig. 8. However, our analyses are based on full month of data. The quoted number below each point represents root mean square error (RMSE) for each case, with the same color scheme used on the plot.

#### 7.3.1 ORDY-BC

In these time series plots, we, once again, found the surface ozone in ORDY-BC is over predicted in January and June (i.e. top and middle panels) and it is in agreement with

Title Page

Abstract

Introduction

Conclusions

References

Tables

Figures



Back

Close

Full Screen / Esc

Printer-friendly Version

Interactive Discussion



our results early in Fig. 7. In comparisons of RMSE, ORDY-BC has shown the worst prediction of surface ozone comparing with others. The RMSE reaches as much as 23.0 ppbv. The highest RMSE occurs at the conditions where the tropopause is low in January and at “near Boulder” site (top left panel). This large RMSE strongly ties to the parameters such as air temperature, altitudinal and latitudinal locations. Since “near Boulder” is located much higher in altitude (i.e. Boulder at about 1650 m a.s.l.) than Huntsville and Trinidad head, larger amount and quicker downshift of uncontrolled stratospheric ozone is expected at the surface of ORDY-BC. This does not happened in Profile-BC and Tropo-BC since both of them do not contain any stratospheric ozone. For air temperature, January has much lower air temperature than June and July. With the relationship of air temperature is direct proportional to tropopause height, lower air temperature means a lower tropopause height. Therefore, a larger amount of aloft ozone is included in the lateral boundary condition of ORDY-BC and results from a huge over prediction of surface ozone in “near Boulder”. This low temperature effect has also contributed to the high RMSE found in “near Huntsville” and “near Trinidad head” sites in January.

Another high RMSE(s) are found in “near Boulder” and “near Trinidad head” in June. These high RMSE(s) most likely relate to the low tropopause height resulting from low air temperature. We believe latitudinal location might explain why “near Boulder” and “near Trinidad head” observed high RMSE, where as “near Huntsville” do not. In general, the higher latitudinal location is, the lower temperature will be when it further away from equator. The low temperature condition affects downscaling process by changing the tropopause height and resulting more stratospheric ozone into the lateral boundary conditions in ORDY-BC. For demonstrating the effect of tropopause due to air temperature and latitudinal location, we have calculated the RMSE in all CASTNET sites for each boundary condition. Moreover, we subtracted the RSME in ORDY-BC to the RSME in Tropo-BC to yield a net RSME for accounting for stratospheric ozone effect, denoted as NET-RSME. Note that the different between ORDY-BC and Tropo-BC is the extra stratospheric concentrations from GEOS-Chem. Therefore, we use the differ-

---

**Techniques for global and regional air quality modeling**Y. F. Lam and J. S. Fu

---

[Title Page](#)[Abstract](#)[Introduction](#)[Conclusions](#)[References](#)[Tables](#)[Figures](#)[◀](#)[▶](#)[◀](#)[▶](#)[Back](#)[Close](#)[Full Screen / Esc](#)[Printer-friendly Version](#)[Interactive Discussion](#)

ences in RMSE as an indicator for stratospheric effects on surface ozone performance. Multivariate statistical fitting is performed on NET-RMSE with monthly average column temperature and latitudinal location. Figure 9 shows the results from statistical analyses: a) Multivariate fitting for NET-RMSE on each month, b) sensitivity analysis on multivariate fitting for month of June. Note that the equations on top of Fig. 9a). are the best-fit equations for temperature and latitude. These equations are used to generate the NET-RMSE predicted in Fig. 9a). and it does not represent the best-fit equations for the straight lines shown in Fig. 9a). For January, NET-RMSE is highly correlated with latitudinal location and air temperature with  $R^2$  of 0.73 and RMSE of 2.73. For June, only air temperature is correlated to NET-RMSE with  $R^2$  of 0.3. And for July, no correlation is found on either latitudinal location or air temperature. Since NET-RMSE is an indicator of the stratospheric effect from the lateral BCs, we believed that no correlation observed in July implies the average column air temperature has reached a certain level at which tropopause height is higher than the upper boundary of CMAQ. Thus, no stratospheric ozone is included in the lateral BCs. To determine the temperature at which no stratospheric effect, we have performed sensitive fittings on June's data because it contains both stratospheric effect sites and non-stratospheric effect sites. Figure 9b shows the results of the sensitive test and the observed break point temperature is about 252 K, at which the lowest RMSE and the highest  $R^2$  are obtained. These results consistent with our early explanations of why bad predictions of ORDY-BC are occurred in January and June and similar predictions as Tropo-BC are found in July. Table 2 shows the monthly average column temperature along with NET-RMSE in all three ozonesonde sites for all months. For January, all three sites have the average temperature lower than 252 K. Therefore, a large NET-RMSE caused from stratospheric ozone is expected. For June, Boulder and Trinidad head are equal or below 252 K, where as Huntsville is above 252 K. Hence, a large NET-RMSE(s) are observed in those two sites and a small NET-RMSE is found in Huntsville. These results are in agreement with our conclusions made early on the time-series plots in Fig. 8. Overall, these results revive the important relationship of temperature and seasonal changes in

---

**Techniques for global and regional air quality modeling**Y. F. Lam and J. S. Fu

---

[Title Page](#)[Abstract](#)[Introduction](#)[Conclusions](#)[References](#)[Tables](#)[Figures](#)[⏪](#)[⏩](#)[◀](#)[▶](#)[Back](#)[Close](#)[Full Screen / Esc](#)[Printer-friendly Version](#)[Interactive Discussion](#)

the GCM downscaling process.

### 7.3.2 Profile-BC

For Profile-BC verse lateral boundary conditions from GCTM, Tang et al. have found that the performance of boundary conditions from GCTM may not necessary better than Profile-BC. Moreover, different GCTM outputs also yield different results. The performance of lateral boundary conditions from GTCM (GCTM-LBC) highly depends on locations and scenarios of the GCTM-LBC, also the type of GCTM used. Al-Saadi et al. suggested that this phenomenon might relate to the ozone aloft in GCTM-LBC, where rapid transports of stratospheric ozone into surface level are observed. In addition, they have found that GCTM-LBC enhances the model errors of ozone concentration at the surface in range of 6 to 20 ppbv in Trinidad Head on August. Since these studies have selected summer ozone season (i.e. August) as their study period, we expect the effect of stratospheric ozone should be minimal based on the relationship we developed early. However, this does not happen. In this case, we suspect their average column temperature in August for Trinidad head may not hot enough to exclude the stratospheric ozone from GCTM-LBC interpolating process. Or may be affected by the quality of GCTM-LBC as inputs where strong boundary influx of ozone affects the simulation results. Nevertheless, these researches have revived that GCTM-LBC preprocessing may be required. In our study, we have implemented tropopause-determining algorithm as the preprocessor for generating ORDY-BC and denoted at Tropo-BC. Note that ORDY-BC is one kind of GCTM-LBC. The intention of the tropopause algorithm is attempting to improve the ozone simulation at the surface. Figure 8 shows the RMSE for both Profile-BC and Tropo-BC. The results shown that the RMSE in Profile-BC is always higher than the RMSE in Tropo-BC, where as the ORDY-BC have either greater or less than Profile BC depended on the locations. Although these differences between Profile-BC and Tropo-BC in RMSE is found within 1 to 2 ppbv in June and July and 3 to 4 ppbv in January, the results have demonstrated the tropopause-determining algorithm has successfully preventing the high surface ozone estimates, in which Tang and

## Techniques for global and regional air quality modeling

Y. F. Lam and J. S. Fu

Title Page

Abstract

Introduction

Conclusions

References

Tables

Figures

◀

▶

◀

▶

Back

Close

Full Screen / Esc

Printer-friendly Version

Interactive Discussion



Al-Saadi mentioned in their study.

### 7.3.3 Tropo-BC

For overall performance of Tropo-BC, we have included additional statistical analyses using all CASTNET data. Table 3 shows the summary of RMSE and mean bias (MB) for all three BCs. In the table, we have broken down the entire US into three regions, which are West Coast (West), Central US (Central) and East Coast (East). The average RMSE for all three months in all stations are calculated to be 14.2 ppbv, 13.3 ppbv and 17.6 ppbv for Profile-BC, Tropo-BC and ORDY-BC, respectively. It is observed that the RMSE in Tropo-BC is always lower than both Profile-BC and ORDY-BC for every region and every month. This demonstrates the Tropo-BC is the best method of generating lateral boundary condition for CMAQ. In the table, large differences (i.e. average in 3 ppbv) between Tropo-BC and Profile-BC are observed in the “West”. It should be noted that this large RMSE improvement in the “West” mainly contributes by the sites that are located in State of Washington. The magnitude of changing RMSE in State of Washington ranges from 4 to 12 ppbv. The poor performance of Profile-BC in RMSE in the “West” has shown that Profile-BC has failed to estimate the impact from intercontinental transport of air pollutants from East Asia through Pacific Ocean. Moreover, it fails to represent the actual geospatial variations of lateral boundary in US.

For the performance of Tropo-BC in all other regions, minor improvement is observed when comparing with Profile-BC. Large improvement is found in month of January. Since Profile-BC uses a fixed BCs and these fixed BCs is usually higher than the actual background ozone in winter, as a result, overestimation of surface ozone in Profile-BC is observed. This demonstrates the importance of using dynamic BCs instead of the static BCs. Figure 10 shows the distributions of RMSE differences among these three scenarios for each CASTNET sites. If we consider  $\pm 1$  ppbv as model variability, then we conclude that only 5% or less of the sites in Tropo-BC have poorer performance comparing with Profile-BC. In these 5% of the sites, we have observed the Tropo-BC overestimated the nighttime ozone concentration in June.

## Techniques for global and regional air quality modeling

Y. F. Lam and J. S. Fu

Title Page

Abstract

Introduction

Conclusions

References

Tables

Figures

◀

▶

◀

▶

Back

Close

Full Screen / Esc

Printer-friendly Version

Interactive Discussion



In comparison with ORDY-BC, Tropo-BC is outperformed for every observation sites in January. Strong improvement in Tropo-BC is found in both January and June. In the plot, we have observed 10% or less of the sites in Tropo-BC have poorer performance than in ORDY-BC (i.e. right side panel). We believed that these 10% is contributed by the nature of underestimation of ozone in 36 km resolution. Since the surface ozone in ORDY-BC is always higher than in Tropo-BC, the improvement may not actually be counted. For the overall performance, Tropo-BC has outperformed ORDY-BC in every month for all regions. These results, once again, demonstrate that the removal of stratospheric ozone using our tropopause-determining algorithm strongly improving the performance of surface ozone simulations in CMAQ.

## 8 Conclusions

In this study, we have successfully integrated our newly developed tropopause-determining algorithm into the methodology of downscaling from global chemical model (i.e. GEOS-Chem) into regional air quality model (i.e. CMAQ). The algorithm searches tropopause height from GCTM outputs and applies tropopause ozone concentration as the maximum ozone concentration at the CMAQ lateral boundary condition. As a result, it excludes any stratospheric ozone from including into regional air quality model. Since CMAQ is only designed for tropospheric application with no top boundary input, any stratospheric ozone or stratospheric intrusion should consider inapplicable in CMAQ. In our results, we have found that the GCTM output (i.e. GEOS-Chem) with the tropopause-determining algorithm (i.e. Tropo-BC) always yield a better result than that with the fixed BCs (i.e. Profile-BC). Moreover, Tropo-BC also yields better results than that with the GCM BCs (i.e. ORDY-BC). For Profile-BC, we have observed the fixed BCs tend to overestimate surface ozone concentration during wintertime and underestimate in summertime. For ORDY-BC, strong over prediction of surface ozone is observed as a result of stratospheric ozone from the upper atmosphere. These results similar to the founding in Tang et al., where a large overestimation is observed in CMAQ surface

## Techniques for global and regional air quality modeling

Y. F. Lam and J. S. Fu

Title Page

Abstract

Introduction

Conclusions

References

Tables

Figures

◀

▶

◀

▶

Back

Close

Full Screen / Esc

Printer-friendly Version

Interactive Discussion



ozone when applying GCTM-BC. Fortunately, with our new tropopause algorithm technique (i.e. Tropo-BC) from the global model input (i.e. GEOS-Chem), we have resolved the high surface ozone issue observed in GCTM-BC, while maintaining good vertical ozone prediction in the upper air. In statistical analysis, we have performed correlation study on average tropospheric column temperature and stratospheric effect using the RMSE differences between ORDY-BC and Tropo-BC. The results show that a break point temperature, in which separates the temperature region between stratospheric effect and non-stratospheric effect, is about 252 K. This value can be used as a quick check to see whether particular region or day having stratospheric effect in GCTM-BC. Nevertheless, this temperature is based on statistical analysis and may contain certain statistical errors. Therefore, we recommend only using this value as a screen tool. In conclusion, we have demonstrated the advantage of using tropopause-determining algorithm along with time-varying GCTM lateral BC for air quality predictions of tropospheric ozone. We have advanced the exiting technique on how GCTM data to be ingesting into CMAQ lateral BC. This methodology can be applied on different GCTM data for downscaling purpose to yield a better surface ozone prediction in a regional CTM.

*Acknowledgements.* This work was supported by the US Environmental Protection Agency under STAR Agreement R830959. It has not formally been reviewed by the EPA. The views presents in this document are solely those of the authors and the EPA does not endorse any products or commercial services mentioned in this publication.

## References

- Al-Saadi, J., Pierce, B., McQueen, J., Natarajan, M., Kuhl, D., Tang, Y. H., Schaack, T. K., and Grell, G.: Global Forecasting System (GFS) Project: Improving National chemistry forecasting and assimilation capabilities, Applications of Environmental Remote Sensing to Air Quality and Public Health, Potomac, MD, May 8–9, 2007.
- Bertschi, I. T., Jaffe, D. A., Jaegle, L., Price, H. U., and Dennison, J. B.: 2002 airborne observations of transpacific transport of ozone, CO, volatile organic compounds, and aerosols to

16032

## Techniques for global and regional air quality modeling

Y. F. Lam and J. S. Fu

Title Page

Abstract

Introduction

Conclusions

References

Tables

Figures

◀

▶

◀

▶

Back

Close

Full Screen / Esc

Printer-friendly Version

Interactive Discussion



---

**Techniques for global  
and regional air  
quality modeling**Y. F. Lam and J. S. Fu

---

[Title Page](#)[Abstract](#)[Introduction](#)[Conclusions](#)[References](#)[Tables](#)[Figures](#)[◀](#)[▶](#)[◀](#)[▶](#)[Back](#)[Close](#)[Full Screen / Esc](#)[Printer-friendly Version](#)[Interactive Discussion](#)

the northeast Pacific: Impacts of Asian anthropogenic and Siberian boreal fire emissions, *J. Geophys. Res.*, 109, D23S12, doi:10.1029/2003JD004328, 2004.

Bethan, S., Vaughan, G., and Reid, S. J.: A comparison of ozone and thermal tropopause heights and the impact of tropopause definition on quantifying the ozone content of the troposphere, *Q. J. Roy. Meteor. Soc.*, 122, 929–944, 1996.

Byun, D. and Schere, K. L.: Review of the governing equations, computational algorithms, and other components of the models-3 Community Multiscale Air Quality (CMAQ) modeling system, *Appl. Mech. Rev.*, 59, 51–77, 2006.

Byun, D. W., Moon, N. K., Jacob, D., and Park, R.: Regional transport study of air pollutants with linked global tropospheric chemistry and regional air quality models, 2nd ICAP Workshop, Research Triangle Park, NC, 2004.

Chin, M., Diehl, T., Ginoux, P., and Malm, W.: Intercontinental transport of pollution and dust aerosols: implications for regional air quality, *Atmos. Chem. Phys.*, 7, 5501–5517, 2007, <http://www.atmos-chem-phys.net/7/5501/2007/>.

Collins, W. J., Derwent, R. G., Garnier, B., Johnson, C. E., Sanderson, M. G., and Stevenson, D. S.: Effect of stratosphere-troposphere exchange on the future tropospheric ozone trend, *J. Geophys. Res.*, 108(D12), 8528, doi:10.1029/2002JD002617, 2003.

Eder, B. and Yu, S. C.: A performance evaluation of the 2004 release of Models-3 CMAQ, *Atmos. Environ.*, 40, 4811–4824, 2006.

Fiore, A., Jacob, D. J., Liu, H., Yantosca, R. M., Fairlie, T. D., and Li, Q.: Variability in surface ozone background over the United States: Implications for air quality policy, *J. Geophys. Res.*, 108(D24), 4787, doi:10.1029/2003JD003855, 2003.

Fu, J. S., Jang, C. J., Streets, D. G., Li, Z. P., Kwok, R., Park, R., and Han, Z. W.: MICS-Asia II: Modeling gaseous pollutants and evaluating an advanced modeling system over East Asia, *Atmos. Environ.*, 42, 3571–3583, 2008.

Fusco, A. C. and Logan, J. A.: Analysis of 1970–1995 trends in tropospheric ozone at Northern Hemisphere midlatitudes with the GEOS-CHEM model, *J. Geophys. Res.*, 108(D15), 4449, doi:10.1029/2002JD002742, 2003.

Heald, C. L., Jacob, D. J., Fiore, A. M., Emmons, L. K., Gille, J. C., Deeter, M. N., Warner, J., Edwards, D. P., Crawford, J. H., Hamlin, A. J., Sachse, G. W., Browell, E. V., Avery, M. A., Vay, S. A., Westberg, D. J., Blake, D. R., Singh, H. B., Sandholm, S. T., Talbot, R. W., and Fuelberg, H. E.: Asian outflow and trans-Pacific transport of carbon monoxide and ozone pollution: An integrated satellite, aircraft, and model perspective, *J. Geophys. Res.*, 108(D24),

4804, doi:10.1029/2003JD003507, 2003.

Heald, C. L., Jacob, D. J., Park, R. J., Alexander, B., Fairlie, T. D., Yantosca, R. M., and Chu, D. A.: Transpacific transport of Asian anthropogenic aerosols and its impact on surface air quality in the United States, *J. Geophys. Res.*, 111, D14310, doi:10.1029/2005JD006847, 2006.

Hoinka, K. P.: The tropopause: discovery, definition and demarcation, *Meteorol. Z.*, 6, 281–303, 1997.

Holton, J. R., Haynes, P. H., McIntyre, M. E., Douglass, A. R., Rood, R. B., and Pfister, L.: Stratosphere-Troposphere Exchange, *Rev. Geophys.*, 33, 403–439, 1995.

Lam, Y. F., Fu, J. S., Gao, Y., Jacob, D., and Park, R.: Downscaling effects of GEOS-Chem as CMAQ initial and boundary conditions: “Tropopause effect”, The 7th Annual CMAS Conference, Chapel Hill, NC, 2008.

Li, Z., Fu, J. S., Jang, C., Wang, B., Mathur, R., Park, R., and Jacob, D.: Evaluation of GEOS-CHEM/CMAQ interface over China and US, The 2nd GEOS-Chem Users’ Meeting, Cambridge MA, April, 2005.

Liang, Q., Jaegle, L., Hudman, R. C., Turquety, S., Jacob, D. J., Avery, M. A., Browell, E. V., Sachse, G. W., Blake, D. R., Brune, W., Ren, X., Cohen, R. C., Dibb, J. E., Fried, A., Fuelberg, H., Porter, M., Heikes, B. G., Huey, G., Singh, H. B., and Wennberg, P. O.: Summertime influence of Asian pollution in the free troposphere over North America, *J. Geophys. Res.*, 112, D12S11, doi:10.1029/2006JD007919, 2007.

Lin, J. T., Wuebbles, D. J., and Liang, X. Z.: Effects of intercontinental transport on surface ozone over the United States: Present and future assessment with a global model, *Geophys. Res. Lett.*, 35, L02805, doi:10.1029/2007GL031415, 2008.

Liu, X., Chance, K., Sioris, C. E., Kurosu, T. P., Spurr, R. J. D., Martin, R. V., Fu, T. M., Logan, J. A., Jacob, D. J., Palmer, P. I., Newchurch, M. J., Megretskaia, I. A., and Chatfield, R. B.: First directly retrieved global distribution of tropospheric column ozone from GOME: Comparison with the GEOS-CHEM model, *J. Geophys. Res.*, 111, D02308, doi:10.1029/2005JD006564, 2006.

Martin, R. V., Jacob, D. J., Logan, J. A., Bey, I., Yantosca, R. M., Staudt, A. C., Li, Q. B., Fiore, A. M., Duncan, B. N., Liu, H. Y., Ginoux, P., and Thouret, V.: Interpretation of TOMS observations of tropical tropospheric ozone with a global model and in situ observations, *J. Geophys. Res.*, 107, D18, 4351, doi:10.1029/2001JD001480, 2002.

Mathur, R., Lin, H. M., McKeen, S., Kang, D., and Wong, D.: Three-dimensional model studies

**Techniques for global and regional air quality modeling**

Y. F. Lam and J. S. Fu

Title Page

Abstract

Introduction

Conclusions

References

Tables

Figures



Back

Close

Full Screen / Esc

Printer-friendly Version

Interactive Discussion



---

**Techniques for global  
and regional air  
quality modeling**Y. F. Lam and J. S. Fu

---

of exchange processes in the troposphere: use of potential vorticity to specify aloft O3 in regional models, The 7th Annual CMAS Conference, Chapel Hill, NC, 2008.

McPeters, R. D., Labow, G. J., and Logan, J. A.: Ozone climatological profiles for satellite retrieval algorithms, *J. Geophys. Res.*, 112, D05308, doi:10.1029/2005JD006823, 2007.

5 Morris, R. E., McNally, D. E., Tesche, T. W., Tonnesen, G., Boylan, J. W., and Brewer, P.: Preliminary evaluation of the community multiscale air, quality model for 2002 over the southeastern United States, *J. Air Waste Manage.*, 55, 1694–1708, 2005.

Morris, R. E., Koo, B., Tesche, T. W., Loomis, C., Stella, G., Tonnesen, G., and Wang, Z.: VISTAS Emissions and Air Quality Modeling – Phase I Task 6 Report: Modeling Protocol for the VISTAS Phase II Regional Haze Modeling, Novato, CA, 2006.

10 Newchurch, M. J., Ayoub, M. A., Oltmans, S., Johnson, B., and Schmidlin, F. J.: Vertical distribution of ozone at four sites in the United States, *J. Geophys. Res.*, 108(D1), 4031, doi:10.1029/2002JD002059, 2003.

Ordóñez, C., Brunner, D., Staehelin, J., Hadjinicolaou, P., Pyle, J. A., Jonas, M., Wernli, H., and Prevot, A. S. H.: Strong influence of lowermost stratospheric ozone on lower tropospheric background ozone changes over Europe, *Geophys. Res. Lett.*, 34, L07805, doi:10.1029/2006GL029113, 2007.

Park, R. J., Jacob, D. J., Chin, M., and Martin, R. V.: Sources of carbonaceous aerosols over the United States and implications for natural visibility, *J. Geophys. Res.*, 108(D12), 4355, doi:10.1029/2002JD003190, 2003.

20 Park, R. J., Jacob, D. J., Field, B. D., Yantosca, R. M., and Chin, M.: Natural and transboundary pollution influences on sulfate-nitrate-ammonium aerosols in the United States: Implications for policy, *J. Geophys. Res.*, 109, D15204, doi:10.1029/2003JD004473, 2004.

Park, R. J., Jacob, D. J., Kumar, N., and Yantosca, R. M.: Regional visibility statistics in the United States: Natural and transboundary pollution influences, and implications for the Regional Haze Rule, *Atmos. Environ.*, 40, 5405–5423, 2006.

Song, C. K., Byun, D. W., Pierce, R. B., Alsaadi, J. A., Schaack, T. K., and Vukovich, F.: Downscale linkage of global model output for regional chemical transport modeling: Method and general performance, *J. Geophys. Res.*, 113, D08308, doi:10.1029/2007JD008951, 2008.

30 Stohl, A., Bonasoni, P., Cristofanelli, P., Collins, W., Feichter, J., Frank, A., Forster, C., Gerasopoulos, E., Gaggeler, H., James, P., Kentarchos, T., Kromp-Kolb, H., Kruger, B., Land, C., Meloan, J., Papayannis, A., Priller, A., Seibert, P., Sprenger, M., Roelofs, G. J., Scheel, H. E., Schnabel, C., Siegmund, P., Tobler, L., Trickl, T., Wernli, H., Wirth, V., Zanis, P., and Zere-

[Title Page](#)[Abstract](#)[Introduction](#)[Conclusions](#)[References](#)[Tables](#)[Figures](#)[◀](#)[▶](#)[◀](#)[▶](#)[Back](#)[Close](#)[Full Screen / Esc](#)[Printer-friendly Version](#)[Interactive Discussion](#)

---

**Techniques for global  
and regional air  
quality modeling**

---

Y. F. Lam and J. S. Fu

---

[Title Page](#)[Abstract](#)[Introduction](#)[Conclusions](#)[References](#)[Tables](#)[Figures](#)[◀](#)[▶](#)[◀](#)[▶](#)[Back](#)[Close](#)[Full Screen / Esc](#)[Printer-friendly Version](#)[Interactive Discussion](#)

fos, C.: Stratosphere-troposphere exchange: A review, and what we have learned from STACCATO, *J. Geophys. Res.*, 108(D12), 8516, doi:10.1029/2002JD002490, 2003.

Streets, D. G., Fu, J. S., Jang, C. J., Hao, J. M., He, K. B., Tang, X. Y., Zhang, Y. H., Wang, Z. F., Li, Z. P., Zhang, Q., Wang, L. T., Wang, B. Y., and Yu, C.: Air quality during the 2008 Beijing Olympic Games, *Atmos. Environ.*, 41, 480–492, 2007.

Tagaris, E., Manomaiphiboon, K., Liao, K. J., Leung, L. R., Woo, J. H., He, S., Amar, P., and Russell, A. G.: Impacts of global climate change and emissions on regional ozone and fine particulate matter concentrations over the United States, *J. Geophys. Res.*, 112, D14312, doi:10.1029/2006JD008262, 2007.

Tang, Y. H., Carmichael, G. R., Thongboonchoo, N., Chai, T. F., Horowitz, L. W., Pierce, R. B., Al-Saadi, J. A., Pfister, G., Vukovich, J. M., Avery, M. A., Sachse, G. W., Ryerson, T. B., Holloway, J. S., Atlas, E. L., Flocke, F. M., Weber, R. J., Huey, L. G., Dibb, J. E., Streets, D. G., and Brune, W. H.: Influence of lateral and top boundary conditions on regional air quality prediction: A multiscale study coupling regional and global chemical transport models, *J. Geophys. Res.*, 112, D10S18, doi:10.1029/2006JD007515, 2007.

Tang, Y. H., Lee, P., Tsidulko, M., Huang, H. C., McQueen, J. T., DiMego, G. J., Emmons, L. K., Pierce, R. B., Thompson, A. M., Lin, H. M., Kang, D., Tong, D., Yu, S. C., Mathur, R., Pleim, J. E., Otte, T. L., Pouliot, G., Young, J. O., Schere, K. L., Davidson, P. M., and Stajner, I.: The impact of chemical lateral boundary conditions on CMAQ predictions of tropospheric ozone over the continental United States, *Environ. Fluid Mech.*, 9(1), 43–58, doi:10.1007/s10652-008-9092-5, 2008.

Tesche, T. W., Morris, R., Tonnesen, G., McNally, D., Boylan, J., and Brewer, P.: CMAQ/CAMx annual 2002 performance evaluation over the eastern US, *Atmos. Environ.*, 40, 4906–4919, 2006.

Vingarzan, R.: A review of surface ozone background levels and trends, *Atmos. Environ.*, 38, 3431–3442, 2004.

WMO: Atmospheric ozone, 1985: WMO Global Ozone Res. and Monit. Proj. Rep. 20, World Meteorological Organization (WMO), Geneva, 1986.

**Table 1.** MM5 and CMAQ model configurations for 2002 simulations.

MM5 configuration	
Model version	3.7
Number of sigma level	34
Number of grid	156×120
Horizontal resolution	36 km
Map projection	Lambert conformal
FDDA	Analysis nudging
Cumulus	Kain-Fritsch 2
Microphysics	Mix-phase
Radiation	RRTM
PBL	Pleim-Xiu
LSM	Pleim-Xiu LSM
LULC	USGS 25-Category

CMAQ configuration	
Model version	4.5
Number of layer	19
Number of grid	148×112
Horizontal resolution	36 km
Horizontal advection	PPM
Vertical advection	PPM
Aerosol module	AERO3
Aqueous module	CB-IV
Emission	VISTAS emissions (NEI 2002 G)
Boundary condition I	CMAQ Predefined Vertical Profile
Boundary condition II	2002 GEOS-Chem

**Techniques for global and regional air quality modeling**

Y. F. Lam and J. S. Fu

Title Page

Abstract

Introduction

Conclusions

References

Tables

Figures



Back

Close

Full Screen / Esc

Printer-friendly Version

Interactive Discussion



## Techniques for global and regional air quality modeling

Y. F. Lam and J. S. Fu

**Table 2.** Summary of NET-RMSE and average column temperatures for the sonde sites.

	Boulder, CO	Huntsville, AL	Trinidad head, CA
January	$T_c = 236$ K NET-RMSE = 10.5 ppbv	$T_c = 246$ K NET-RMSE = 11.4 ppbv	$T_c = 242$ K NET-RMSE = 6.9 ppbv
June	$T_c = 247$ K NET-RMSE = 6.5 ppbv	$T_c = 254$ K NET-RMSE = 1.4 ppbv	$T_c = 252$ K NET-RMSE = 7.9 ppbv
July	$T_c = 253$ K NET-RMSE = 0.39 ppbv	$T_c = 257$ K NET-RMSE = 1.0 ppbv	$T_c = 255$ K NET-RMSE = 0.1 ppbv

$T_c$  is average vertical column temperature; NET-RMSE is the RMSE difference between Profile-BC and Tropo-BC

Title Page

Abstract

Introduction

Conclusions

References

Tables

Figures

◀

▶

◀

▶

Back

Close

Full Screen / Esc

Printer-friendly Version

Interactive Discussion



**Table 3.** Summary of NET-RMSE and average column temperatures for the sonde sites.

		Profile-BC	Tropo-BC	ORDY-BC
January	ALL	RMSE = 11.9 ppbv MB = 7.3 ppbv	RMSE = 10.3 ppbv MB = 3.9 ppbv	RMSE = 19.8 ppbv MB = 13.2 ppbv
	WEST	RMSE = 16.8 ppbv MB = 14.6 ppbv	RMSE = 13.0 ppbv MB = 9.8 ppbv	RMSE = 23.5 ppbv MB = 18.3 ppbv
	CENTRAL	RMSE = 10.1 ppbv MB = 6.6 ppbv	RMSE = 8.2 ppbv MB = 2.4 ppbv	RMSE = 23.6 ppbv MB = 16.1 ppbv
	EAST	RMSE = 11.2 ppbv MB = 6.3 ppbv	RMSE = 10.1 ppbv MB = 3.2 ppbv	RMSE = 18.0 ppbv MB = 11.5 ppbv
June	ALL	RMSE = 14.3 ppbv MB = 0.3 ppbv	RMSE = 13.8 ppbv MB = 1.9 ppbv	RMSE = 16.4 ppbv MB = 7.2 ppbv
	WEST	RMSE = 18.3 ppbv MB = 4.3 ppbv	RMSE = 15.2 ppbv MB = 2.0 ppbv	RMSE = 19.9 ppbv MB = 7.2 ppbv
	CENTRAL	RMSE = 12.5 ppbv MB = -4.5 ppbv	RMSE = 11.3 ppbv MB = -1.3 ppbv	RMSE = 16.0 ppbv MB = 6.1 ppbv
	EAST	RMSE = 14.1 ppbv MB = 1.1 ppbv	RMSE = 14.1 ppbv MB = 2.9 ppbv	RMSE = 15.9 ppbv MB = 7.6 ppbv
July	ALL	RMSE = 16.3 ppbv MB = 4.2 ppbv	RMSE = 15.8 ppbv MB = 3.4 ppbv	RMSE = 16.6 ppbv MB = 5.3 ppbv
	WEST	RMSE = 19.8 ppbv MB = 4.3 ppbv	RMSE = 16.9 ppbv MB = 4.1 ppbv	RMSE = 16.9 ppbv MB = 6.0 ppbv
	CENTRAL	RMSE = 13.7 ppbv MB = -2.4 ppbv	RMSE = 13.3 ppbv MB = -3.1 ppbv	RMSE = 13.7 ppbv MB = -1.4 ppbv
	EAST	RMSE = 16.4 ppbv MB = 6.2 ppbv	RMSE = 16.3 ppbv MB = 6.1 ppbv	RMSE = 17.3 ppbv MB = 8.1 ppbv

ALL – All stations; WEST – West of 115° W; CENTRAL – Between 115° W and 94° W; EAST – East of 94° W; RMSE is root mean square error; MB is mean bias

**Techniques for global and regional air quality modeling**

Y. F. Lam and J. S. Fu

Title Page

Abstract

Introduction

Conclusions

References

Tables

Figures

◀

▶

◀

▶

Back

Close

Full Screen / Esc

Printer-friendly Version

Interactive Discussion



## Techniques for global and regional air quality modeling

Y. F. Lam and J. S. Fu

**Table A1.** GEOS-Chem to CMAQ IC/BC species mapping table.

CMAQ CB-IV specie	GEOS-CHEM species
[NO <sub>2</sub> ]	[NO <sub>x</sub> ]
[O <sub>3</sub> ]	[O <sub>x</sub> ] – [NO <sub>x</sub> ]
[N <sub>2</sub> O <sub>5</sub> ]	[N <sub>2</sub> O <sub>5</sub> ]
[HNO <sub>3</sub> ]	[HNO <sub>3</sub> ]
[PNA]	[HNO <sub>4</sub> ]
[H <sub>2</sub> O <sub>2</sub> ]	[H <sub>2</sub> O <sub>2</sub> ]
[CO]	[CO]
[PAN]	[PAN] + [PMN] + [PPN]
[MGLY]	[MP]
[ISPD]	[MVK] + [MACR]
[NTR]	1/2 [R4N2]
[FORM]	[CH <sub>2</sub> O]
[ALD2]	[ALD2]+[RCHO]
[PAR]	1/4 [ALK4] + 1/3 [C <sub>3</sub> H <sub>8</sub> ] + 10/4 [C <sub>2</sub> H <sub>6</sub> ] + 1/3 [ACET] + 1/4 [MEK] + 1/2 [PREPE]
[OLE]	1/2 [PRPE]
[ISOP]	1/5 [ISOP]
[SO <sub>2</sub> ]	[SO <sub>2</sub> ]
[NH <sub>3</sub> ]	[NH <sub>3</sub> ]
[ASO <sub>4</sub> J]	[SO <sub>4</sub> ]
[ANH <sub>4</sub> J]	[NH <sub>4</sub> ]
[ANO <sub>3</sub> J]	[NIT]
[AECJ]	[BCPI] + [BCPO]
[AORGP AJ]	[OCPI] + [OCPO]
[AORGBJ]	[SOA1]

Title Page

Abstract

Introduction

Conclusions

References

Tables

Figures

◀

▶

◀

▶

Back

Close

Full Screen / Esc

Printer-friendly Version

Interactive Discussion



**Techniques for global  
and regional air  
quality modeling**

Y. F. Lam and J. S. Fu

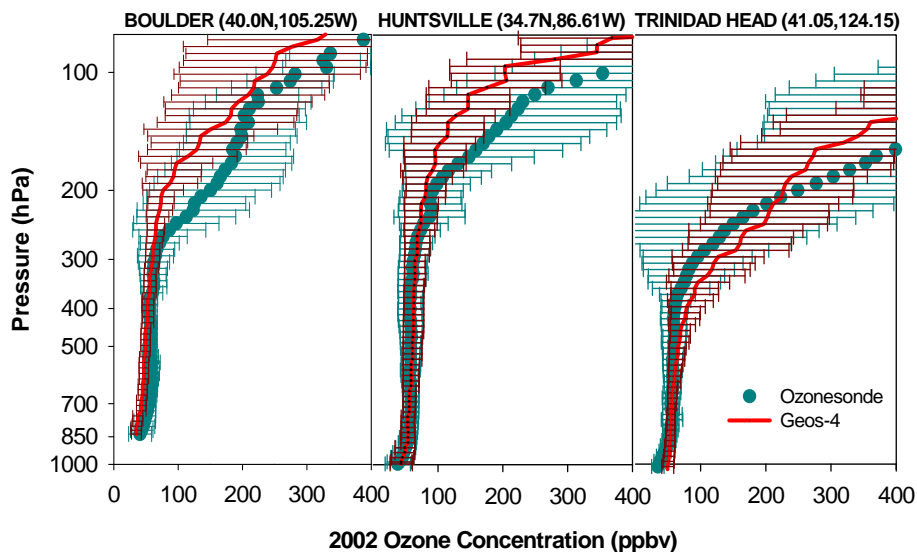


**Fig. 1.** Yearly variability of GEOS-Chem outputs versus ozonesonde.

[Title Page](#)[Abstract](#)[Introduction](#)[Conclusions](#)[References](#)[Tables](#)[Figures](#)[◀](#)[▶](#)[◀](#)[▶](#)[Back](#)[Close](#)[Full Screen / Esc](#)[Printer-friendly Version](#)[Interactive Discussion](#)

**Techniques for global  
and regional air  
quality modeling**

Y. F. Lam and J. S. Fu

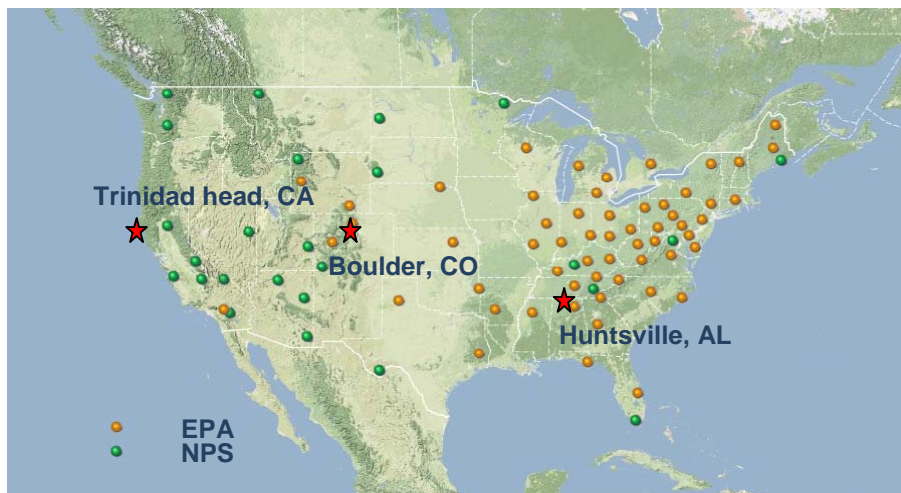


**Fig. 2.** The CONUS domain with observation sites marked in green or orange from CASTNET and ozonesondes in red star.

[Title Page](#)[Abstract](#)[Introduction](#)[Conclusions](#)[References](#)[Tables](#)[Figures](#)[I◀](#)[▶I](#)[◀](#)[▶](#)[Back](#)[Close](#)[Full Screen / Esc](#)[Printer-friendly Version](#)[Interactive Discussion](#)

**Techniques for global  
and regional air  
quality modeling**

Y. F. Lam and J. S. Fu

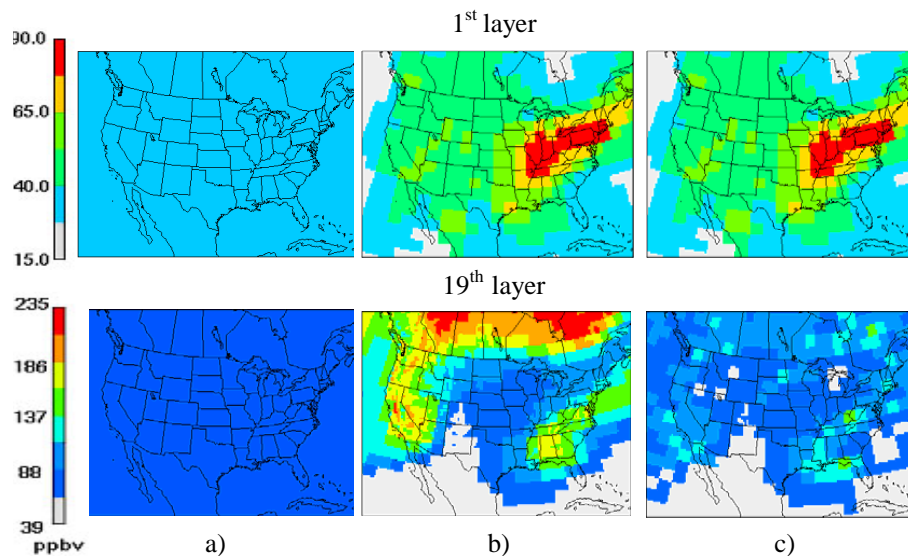


**Fig. 3.** Comparison of different lateral boundary conditions in 1st and 19th layers, **(a)** Profile-BC, **(b)** ORDY-BC, and **(c)** Tropo-BC.

Title Page

Abstract

Introduction

Conclusions

References

Tables

Figures

◀

▶

◀

▶

Back

Close

Full Screen / Esc

Printer-friendly Version

Interactive Discussion



**Techniques for global  
and regional air  
quality modeling**

Y. F. Lam and J. S. Fu

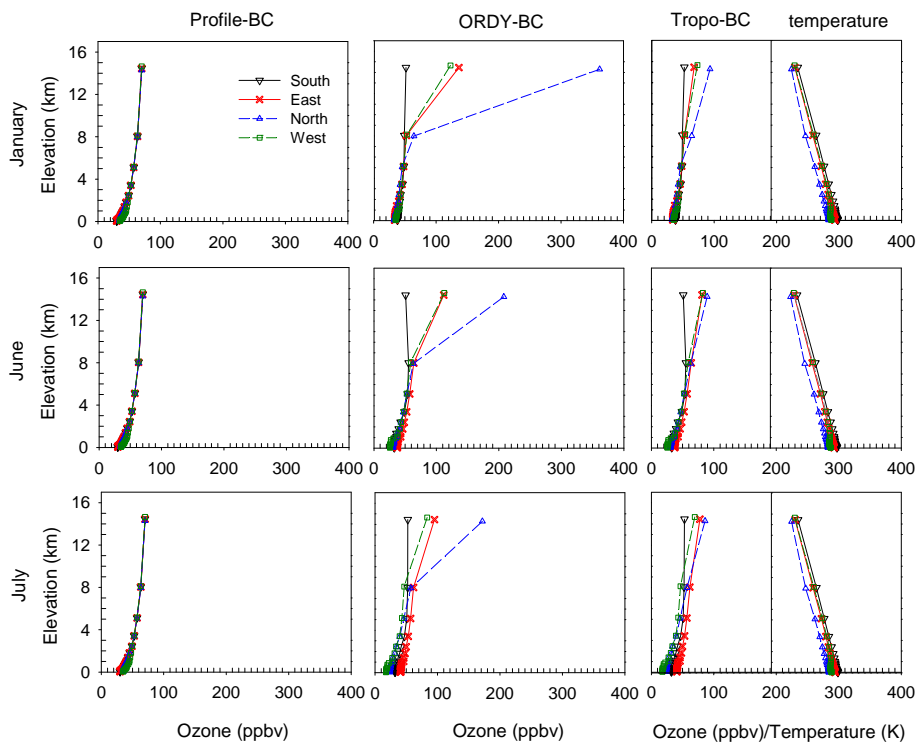


**Fig. 4.** Monthly vertical distribution of ozone from CMAQ BCs: South (black line), East (Red line), North (blue line), and West (green line) of CONUS domain in January, June and July with temperature profiles for Profile-BC (left), ORDY-BC (middle) and Tropo-BC (right).

Title Page

Abstract

Introduction

Conclusions

References

Tables

Figures

◀

▶

◀

▶

Back

Close

Full Screen / Esc

Printer-friendly Version

Interactive Discussion



**Techniques for global  
and regional air  
quality modeling**

Y. F. Lam and J. S. Fu

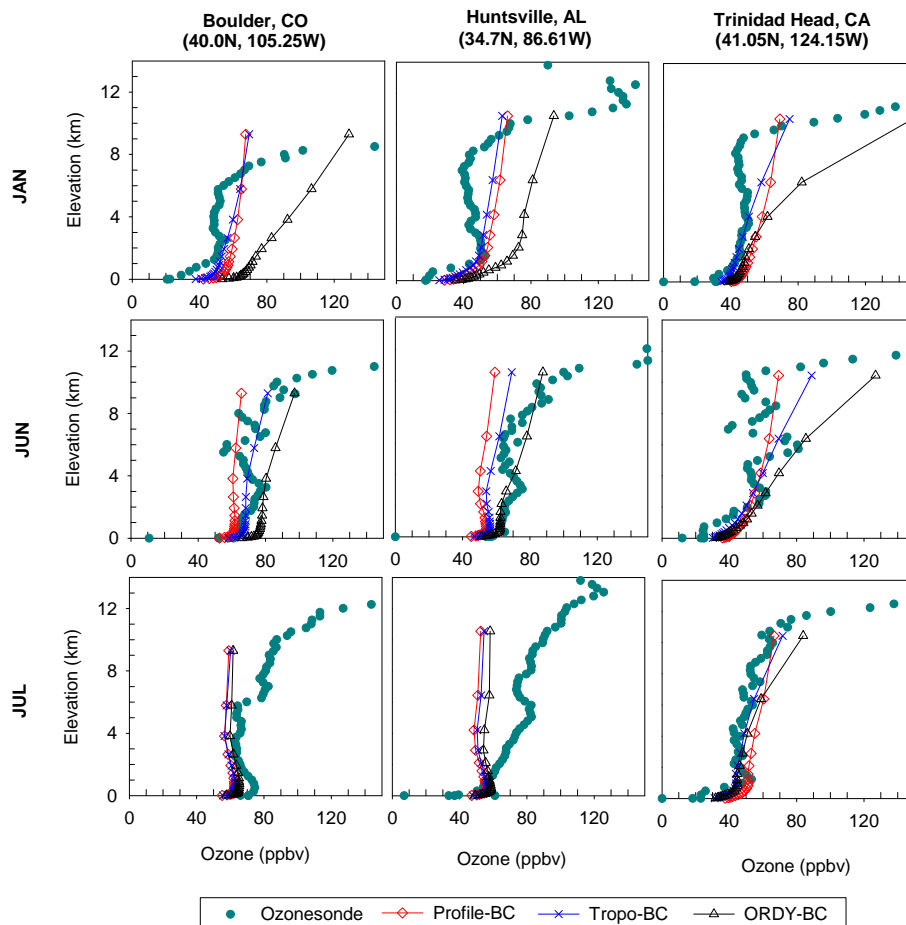


**Fig. 5.** CMAQ simulated monthly vertical distribution of ozone for Profile-BC (red line), Tropo-BC (blue line) and ORDY-BC (black line) with ozonesonde.

Title Page

Abstract

Introduction

Conclusions

References

Tables

Figures

◀

▶

◀

▶

Back

Close

Full Screen / Esc

Printer-friendly Version

Interactive Discussion



**Techniques for global  
and regional air  
quality modeling**

Y. F. Lam and J. S. Fu

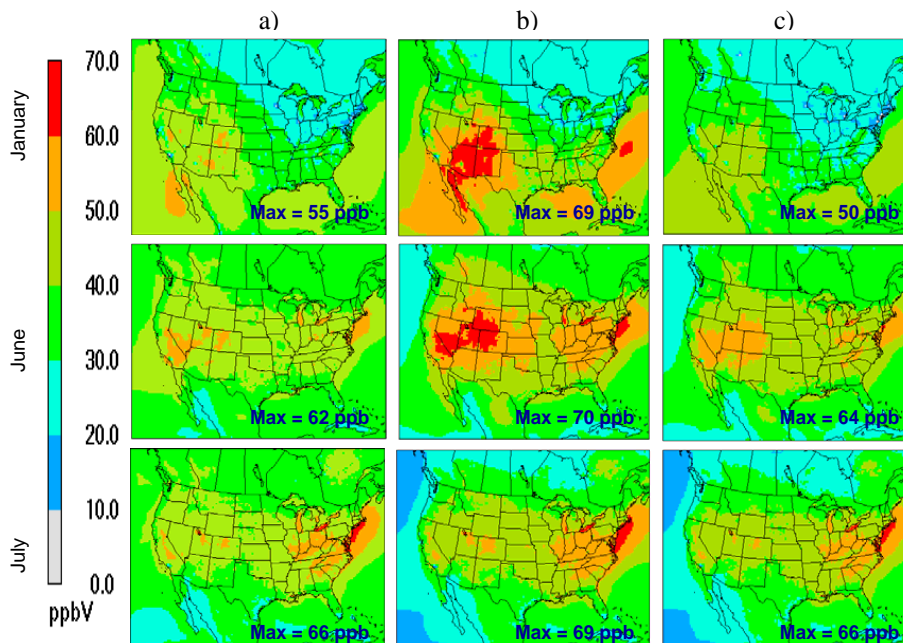


**Fig. 6.** Comparisons of monthly average ozone concentrations in January, June and July from CMAQ outputs; **(a)** Profile-BC (left), **(b)** ORDY-BC (middle), and **(c)** Tropo-BC (right). The maximum concentration within the domain is shown at the bottom of right hand corner.

[Title Page](#)[Abstract](#)[Introduction](#)[Conclusions](#)[References](#)[Tables](#)[Figures](#)[◀](#)[▶](#)[◀](#)[▶](#)[Back](#)[Close](#)[Full Screen / Esc](#)[Printer-friendly Version](#)[Interactive Discussion](#)

Techniques for global  
and regional air  
quality modeling

Y. F. Lam and J. S. Fu

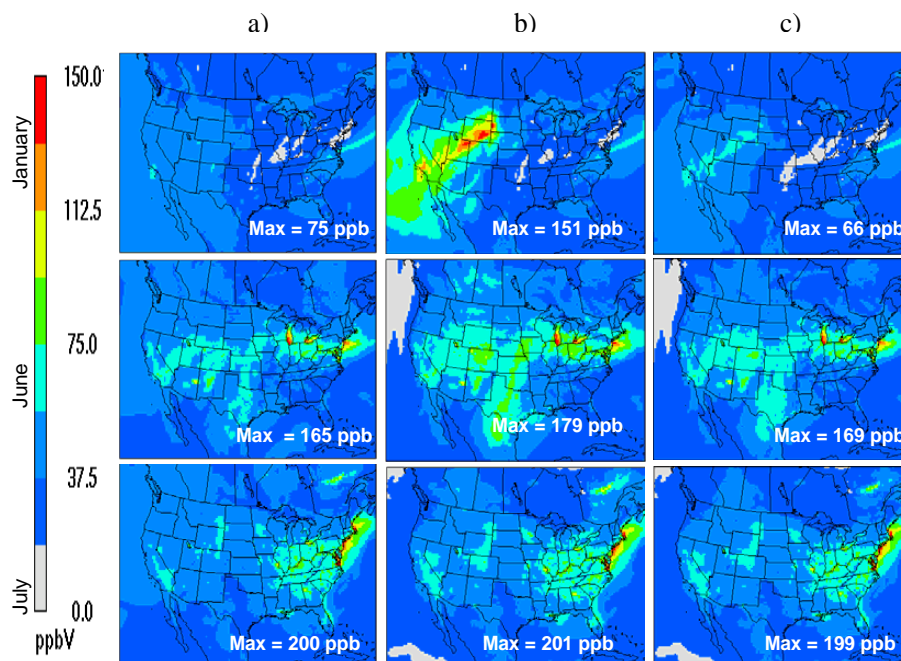


**Fig. 7.** Comparisons of monthly maximum 8-h surface ozone concentrations in January, June and July from CMAQ outputs; **(a)** Profile-BC (left), **(b)** ORDY-BC (middle), and **(c)** Tropo-BC (right). The maximum concentration within the domain is shown at the bottom of right hand corner.

[Title Page](#)[Abstract](#)[Introduction](#)[Conclusions](#)[References](#)[Tables](#)[Figures](#)[◀](#)[▶](#)[◀](#)[▶](#)[Back](#)[Close](#)[Full Screen / Esc](#)[Printer-friendly Version](#)[Interactive Discussion](#)

## Techniques for global and regional air quality modeling

Y. F. Lam and J. S. Fu

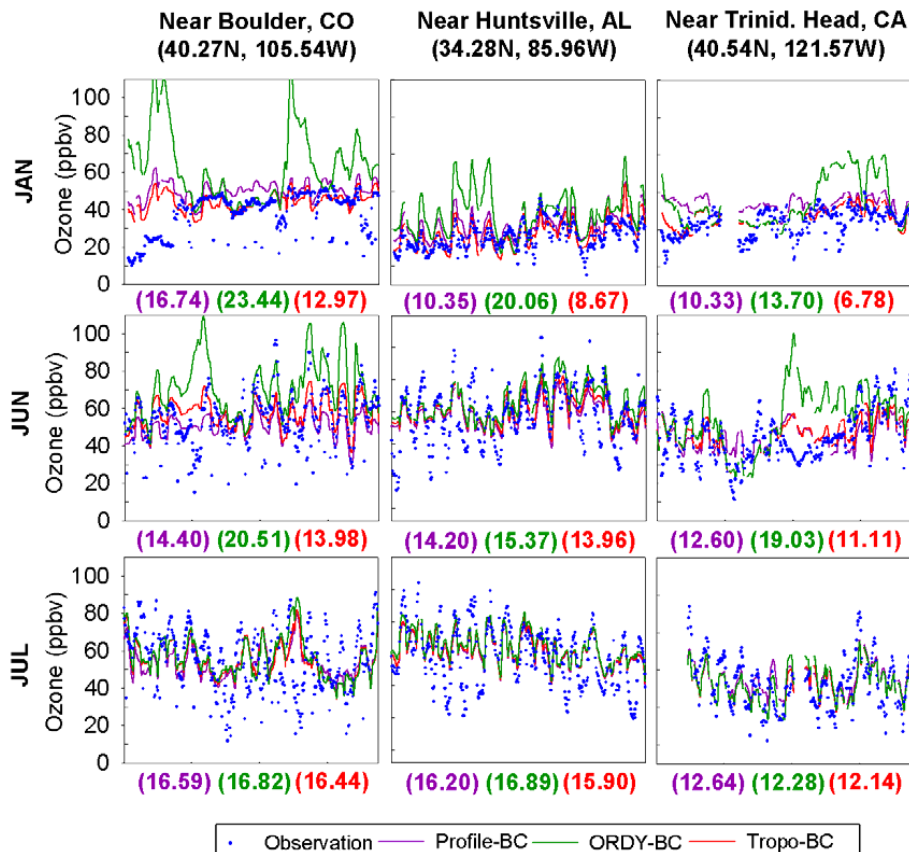


**Fig. 8.** Comparison of simulated and measured surface ozone concentration for month of January, June and July from the selected sites. The quoted value at the bottom of each plot revives the root mean square error of each case.

Title Page

Abstract

Introduction

Conclusions

References

Tables

Figures

◀

▶

◀

▶

Back

Close

Full Screen / Esc

Printer-friendly Version

Interactive Discussion



## Techniques for global and regional air quality modeling

Y. F. Lam and J. S. Fu

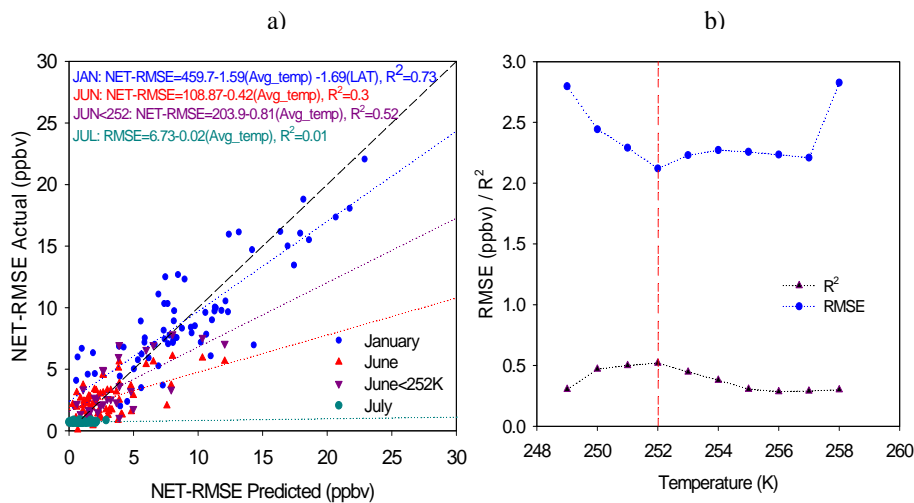


**Fig. 9.** Statistical analysis outputs from CASTNET sites: **(a)** NET-RMSE actual vs. NET-RMSE predicted, **(b)** sensitivity analysis on best-fit equation for June data.

Title Page

Abstract

Introduction

Conclusions

References

Tables

Figures

◀

▶

◀

▶

Back

Close

Full Screen / Esc

Printer-friendly Version

Interactive Discussion



Techniques for global  
and regional air  
quality modeling

Y. F. Lam and J. S. Fu

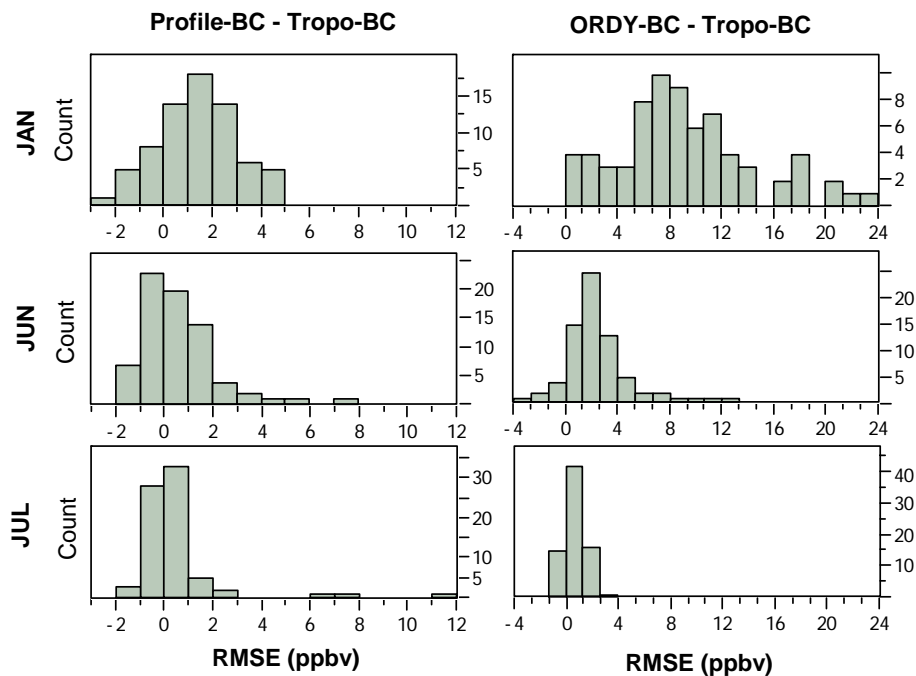


**Fig. 10.** Summary of the RMSE distributions for the differences among these three scenarios for each CASTNET sites.

[Title Page](#)[Abstract](#)[Introduction](#)[Conclusions](#)[References](#)[Tables](#)[Figures](#)[◀](#)[▶](#)[◀](#)[▶](#)[Back](#)[Close](#)[Full Screen / Esc](#)[Printer-friendly Version](#)[Interactive Discussion](#)